Reaction of Chloride Ion with Isopropyl Bromide at Atmospheric Pressure by Ion Mobility Spectrometry

K. E. Sahlstrom, W. B. Knighton, and E. P. Grimsrud*

Department of Chemistry, Montana State University, Bozeman, Montana 59717

Received: July 17, 1996; In Final Form: October 21, 1996[⊗]

The S_N2 nucleophilic displacement reaction of chloride ion with isopropyl bromide (*i*-PrBr) has been studied in nitrogen buffer gas at a pressure of 640 Torr over the temperature range 20−175 °C by ion mobility spectrometry (IMS). It is concluded that, under these conditions of relatively high buffer gas pressure, this nucleophilic displacement reaction occurs primarily by the distinctly two-step mechanism $Cl^- + i\text{-PrBr} \rightleftharpoons Cl^-(i\text{-PrBr}) \rightarrow Br^- + i\text{-PrCl}$ in which a thermal energy ion complex, $Cl^-(i\text{-PrBr})$, is maintained in a state of chemical equilibrium with the reactants. An S_N2 displacement reaction then occurs within the thermal energy cluster ion by its unimolecular conversion to products. Equilibrium constants, K_1, and rate constants, k_1, for $Cl^- + i\text{-PrBr} \rightleftharpoons Cl^-(i\text{-PrBr})$ and $Cl^-(i\text{-PrBr}) \rightarrow Br^- + i\text{-PrCl}$, respectively, are determined from the IMS spectra as a function of temperature. In addition, second-order clustering to form the ion complex $Cl^-(i\text{-PrBr})_2$ is also observed, and equilibrium constants, K_2, for this process are also obtained from IMS spectra. By these measurements, the major features of the potential energy surface for this reaction are characterized and place its S_N2 transition state at 1.6 kcal mol^{-1} above the energy of the reactants.

Introduction

While the field of gas phase ion chemistry has received a great deal of attention during the past 3 decades, due to instrumental deficiencies, very few ion−molecule (IM) reactions have been studied in buffer gases of pressure greater than about 10 Torr.[1] A principal motivation for studying gas phase ionic reactions in buffer gases of greater pressure is so that IM reactions can be observed under conditions where all species along the reaction coordinate, including short-lived intermediates as well as reactants, are maintained in a state of thermal equilibrium with the medium. Kinetic behavior under such conditions are of fundamental interest to the field of gas phase ion chemistry and can greatly facilitate the interpretation of kinetic data in terms of the potential energy surfaces of the reactions.[1−5]

We have recently reported the use of ion mobility spectrometry (IMS) for the study of several relatively simple ion−molecule processes occurring in a buffer gas of 1 atm pressure.[1,6−8] For example, we have shown[6,8] that rate constants for various bimolecular reactions, such as the one shown in reaction 1,

$$Cl^- + CH_3Br \rightarrow Br^- + CH_3Cl \qquad (1)$$

can be reliably determined in an atmospheric pressure buffer gas by IMS. We have also shown[7] that equilibrium constants for clustering reactions, such as that shown in reaction 2,

$$Cl^-(CHCl_3)_{n-1} + CHCl_3 = Cl^-(CHCl_3)_n \qquad (2)$$

where $n = 1$ and 2, can be reliably measured at atmospheric pressure by IMS. The average rate constant for the bimolecular reactions of various sets of equilibrated cluster ions, as shown by reaction 3,

$$Cl^-(CHCl_3)_n + CH_3Br \rightarrow Br^-(CHCl_3)_m + CH_3Cl \qquad (3)$$

where n and m vary from 0 to 2, have also been measured by IMS.[7]

In the present investigation, we report the use of the IMS technique to investigate the nucleophilic displacement reaction of chloride ion with isopropyl bromide (*i*-PrBr). As compared to bimolecular reaction 1, the reaction of Cl^- with *i*-PrBr is complicated by two factors. One is that the nucleophilic attack of the chloride ion on this secondary alkyl bromide proceeds much more slowly due to increased steric hindrance expected in its S_N2 transition state. The other is that the enthalpy of association between chloride and isopropyl bromide will be significantly greater so that a significant fraction of the total chloride ion population can be present in the single-clustered form, $Cl^-(i\text{-PrBr})$, and even the double-clustered form, $Cl^-(i\text{-PrBr})_2$, under conditions of low-to-moderate temperatures and relatively high *i*-PrBr concentrations. For these reasons, the reaction of Cl^- with *i*-PrBr is more appropriately represented by reaction sequence 4,

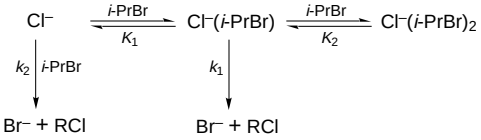

(4)

where the clustering reactions are indicated on the top line with equilibrium constants K_1 and K_2, along with two likely S_N2 reaction pathways. One pathway involves a direct bimolecular reaction of Cl^- ion with *i*-PrBr with second-order rate constant, k_2, and another involves the unimolecular dissociation of the thermalized single-cluster ion, $Cl^-(i\text{-PrBr})$, with first-order rate constant, k_1, to form the displacement products, Br^- and *i*-PrCl. It is recognized that an S_N2 displacement reaction could also occur within the second-order cluster ion, $Cl^-(i\text{-PrBr})_2$, shown in reaction sequence 4. However, it will be assumed here that this third reaction pathway will not be of importance under any conditions used here in which the bare Cl^- ion or the single-clustered ions, $Cl^-(i\text{-PrBr})$, have significant relative abundance. This assumption is supported by the fact that the attachment of neutral molecules to atomic anions such as Cl^- has been shown to greatly reduce the nucleophilic reactivity of the core anion.[7,9−12]

[⊗] Abstract published in *Advance ACS Abstracts,* February 1, 1997.

S1089-5639(96)02167-6 CCC: $14.00

A characterization of the reaction of Cl^- with *i*-PrBr in 4 Torr of methane buffer gas has been previously described by Caldwell, Magnera, and Kebarle (13) using a pulsed electron beam high-pressure mass spectrometer (PHPMS). In that study, rate constants were reported only under relatively high temperature conditions, where the fraction of Cl^- ions held in the *i*-PrBr clustered forms was very small. In this way, their PHPMS measurements could be treated as if the reaction always occurred by a simple bimolecular process, even though Caldwell *et al.* recognized that the actual mechanism might have involved the prior formation of a thermalized ion complex, as shown in reaction sequence 4.

Under the conditions of the present study, it will be shown that equilibrium constants for the clustering reactions and rate constants for the substitution reactions can be simultaneously determined from IMS measurements over a range of temperatures in a near-atmospheric pressure buffer gas. By comparison of the present results obtained in 640 Torr of nitrogen buffer gas (ambient pressure in Bozeman, MT) with those obtained by Caldwell *et al.*[13] in 4 Torr of methane buffer gas, the relative importance of the bimolecular S_N2 mechanism (k_2) and the unimolecular S_N2 mechanism (k_1) shown in reaction 4 under atmospheric pressure conditions will be assessed.

Experimental Section

The IMS instrument has been previously described in detail,[6−8] and only a summary of its operating principles will be provided here. Chloride ions are initially produced in its ^{63}Ni-based ion source by electron capture to CCl_4, which is added in very small quantities (about 10 parts per billion) to the main source gas (nitrogen, atmospheric pressure). Small packets of source-produced Cl^- ions are then allowed to enter the drift region of the IMS by momentarily (0.5 ms) opening a Bradbury−Nielson ion gate. The drift tube contains a counterflowing current of nitrogen gas that prevents the penetration of source gas into the drift region. In the drift tube, all ions are transported through the nitrogen gas at atmospheric pressure to a Faraday detection plate at various rates determined by the mobilities of the individual ions and the applied electric field. The entire IMS instrument is enclosed within an insulated jacket. The temperature of the IMS was increased by electrical heating within the IMS oven and was decreased slightly below ambient temperature when desired by a radiator through which tap water was passed.

During transport through the drift region, the Cl^- ions will undergo various interactions (reaction sequence 4) with isopropyl bromide which is continuously bled into to the nitrogen drift gas from an associated gas handling plant. Chemical interactions of Cl^- with *i*-PrBr within the drift region change the identity and the mobilities of the ions, thereby changing the nature of the observed IMS spectra. Measurements of ion arrival at the Faraday detection plate are made both by an electrometer connected to the Faraday plate and by an associated mass spectrometer that samples the contents of gas leaking through a 50 μm aperture located at the center of the Faraday plate. The Faraday plate electrometer thereby provides a "total" ion mobility spectrum, and the mass spectrometer provides a "single" ion mobility spectrum of any mass-selected ion of interest. It has been shown[6] that a large and constant fraction of all ions within the drift region are transported to the Faraday plate regardless of their mobilities. Therefore, the reaction-modified IMS spectra that is measured at the Faraday plate can be used directly, assuming uniform sensitivity to all ions, for the determination of the relative amounts of reactant ions lost and product ions produced during the transport of an ion packet through the drift region. The associated mass spectrometer is used simply to verify the assignments of individual ions to various portions of the observed total ion IMS spectra. Since the ratio of the drift field (156 V/cm or lower) to the pressure (640 Torr) is relatively low, it can be assumed that the kinetic and internal energy of the ions is not significantly affected by the drift field.[6] Therefore, the equilibrium and rate constants reported here reflect those of thermal energy ions.

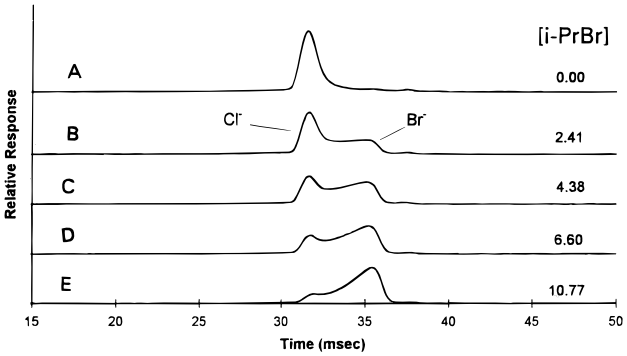

Figure 1. Reaction-modified ion mobility spectra observed at relatively high temperature, 150 °C. The reactant ion, Cl^-, is made in the ion source by electron capture to CCl_4. The product ion, Br^-, is produced at all points along the drift tube by the reaction of Cl^- with *i*-PrBr. The concentration of *i*-BrPr added to the drift tube is indicated (in units of 10^{13} molecules/cm^3). The electric field within the drift tube is 140 V cm^{-1}. Note that the drift times of the ions are not significantly increased by the successive addition of *i*-PrBr to the drift gas at this temperature.

The reagent grade *i*-PrBr (Alltech) that was injected into the GHP was first treated in order to remove any traces of HBr that would have otherwise complicated the present measurements by its fast reaction with Cl^-. This was accomplished by shaking equal volumes of *i*-PrBr with an aqueous solution of saturated $NaHCO_3$ in a separation funnel. After repeating this separation six times, the final volume of *i*-PrBr was dried with $MgSO_4$.

Results and Discussion

Overview of Reaction-Modified IMS Spectra. In characterizing the interactions of chloride ion with isopropyl bromide from IMS data, it is useful to first consider the general nature of reaction-modified IMS spectra obtained at relatively high and then relatively low temperatures. In Figure 1, IMS spectra are shown that reflect the reaction of Cl^- ion with *i*-PrBr under conditions of relatively high temperature, 150 °C. Under these conditions, the IMS spectrum is relatively simple and resembles those reported previously for the reactions of chloride ion with methyl bromide and other primary alkyl bromides.[6,8] As successively greater concentrations of *i*-PrBr are added to the drift tube, the magnitude of the distinct source-generated Cl^- peak decreases while the magnitude of the broad drift-tube-generated Br^- peak increases. The identity of the Cl^- and Br^- ions that contribute to the two portions of the total IMS spectra in Figure 1 was verified by parallel measurements made with the mass spectrometer.[6−8]

From measurements such as shown in Figure 1, a determination of a second-order rate constant for the apparent bimolecular reaction between Cl^- and *i*-PrBr could be obtained, if desired, by analysis of the relative areas underlying the Cl^- and Br^- portions of the reaction-modified total ion IMS spectra shown.[6] A more comprehensive discussion of how rate constants were determined here will be deferred until later, however, while attention is now drawn to the observed drift times of the ions. It is noted in Figure 1 that the drift times of the Cl^- and Br^- ions are almost constant and are increased only slightly by the successive additions of *i*-PrBr to the drift gas at

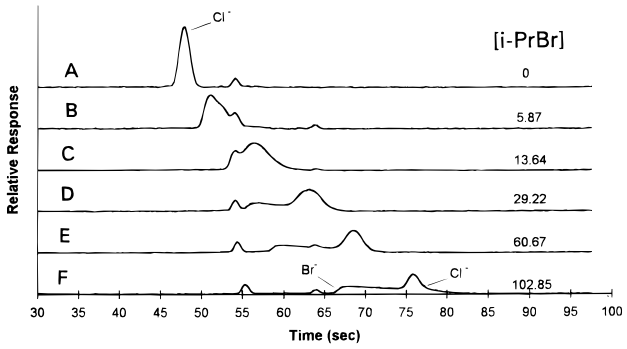

Figure 2. Reaction-modified ion mobility spectra observed at a relatively low temperature, 35 °C, as a function of the *i*-PrBr concentration (in units of 10^{13} molecules cm^{-3}) added to the drift gas. The electric field is 140 V cm^{-1}. At this temperature, the drift times of the Cl^- reactant and Br^- product ions are significantly increased with increased [*i*-PrBr] due to the clustering of both halide ions with *i*-PrBr. At this temperature, additional ions are also noted at drift times of about 55 and 64 ms. These two ions are formed unintentionally in the ion source and are transported through the drift region without change. The identities of the primary ions that contribute to these IMS spectra are provided by associated mass spectrometry measurements, as shown in Figure 3.

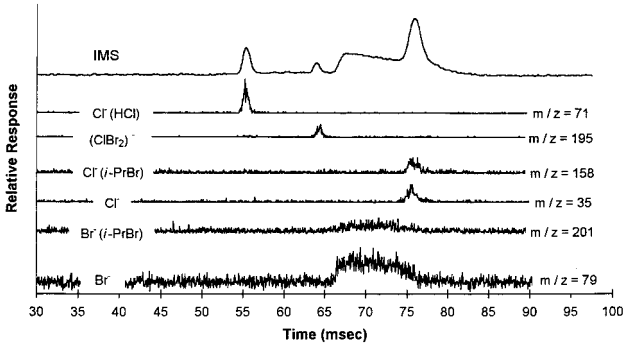

Figure 3. Several single-ion IMS spectra for principal ions that contribute to the total ion IMS spectrum observed for condition F in Figure 2. The ion identities indicated in this figure were confirmed by parallel measurements in which the intensity of other expected ions within the $^{35}Cl/^{37}Cl$ and/or $^{79}Br/^{81}Br$ isotopic cluster groups of each ion type were measured. The origins of all ions indicated here are explained in the text.

150 °C. This indicates that almost all of the chloride and bromide ions are in the unclustered form at 150 °C under all of the conditions shown in Figure 1. In addition, no clustered ions of the types Cl^-(*i*-PrBr) or Br^-(*i*-PrBr) were detected by the mass spectrometer under these conditions.

When analogous experiments were performed at relatively low temperatures, IMS spectra such as those shown in Figure 2 at 35 °C were obtained. These IMS spectra are clearly much more complex than those in Figure 1 and require additional explanation. Again, the magnitude of the peak containing the Cl^- ion decreases continuously as greater amounts of *i*-PrBr are added to the drift gas. In addition, a large shift of the Cl^--containing peak to longer drift times is caused by an increase in the concentration of *i*-PrBr. The Br^--containing ions that are generated in the drift tube are also shifted to longer drift times with increasing amounts of *i*-PrBr, but to a lesser extent than those containing Cl^-. These shifts in drift time cause the Cl^--containing peak to move through and then to the right of the position of the Br^--containing ions within the reaction-modified IMS wave form as successively greater amounts of *i*-PrBr are added to the drift gas.

The identities of the ions that contribute to the total IMS spectra observed at 35 °C are indicated in Figure 3 where numerous mass-selected single-ion IMS measurements are shown under condition F of Figure 2. The identities of the ions that are thought to cause the signals at each *m*/*z* value are also indicated. These identity assignments were verified by parallel measurements (not shown) in which the expected ions of the other abundant isotopes of chlorine and bromine were monitored. The last four IMS spectra in Figure 3 indicate that the shifts in the drift times of the Cl^- and Br^- ions noted in Figure 2 are due to the clustering of these ions with *i*-PrBr. The fact that the bare and clustered halide ions have the same IMS peak shapes and drift times indicates that the clustering of *i*-PrBr to Cl^- and Br^- are very fast processes under these conditions relative to the rates at which these ions are transported through the drift tube.

Additional ions not seen in the IMS spectra at high temperatures are also noted in the IMS experiments performed at low temperature in Figures 2 and 3. At ≈55 ms, an ion which has been identified as Cl^-(HCl) is consistently observed in all IMS spectra at low temperature. This ion appears to be formed only in the ion source by the association of some of the Cl^- ions with a trace quantity of HCl formed by radiation chemistry within the ^{63}Ni ion source. With CCl_4 continuously present in the ion source, the production of trace quantities of HCl appears to be unavoidable. (The source of hydrogen atoms is thought to be water which, in spite of considerable efforts for its removal, is always present at trace levels.) However, as evidenced by the constancy of the intensities and drift times of the Cl^-(HCl) peaks in the IMS spectra in Figure 2, the ion, Cl^-(HCl), appears to undergo no reactions in the drift region. Therefore, this ion is thought to have no affect on the IMS reaction wave form of interest, and its presence was ignored. With use of higher ion source and drift tube temperatures (Figure 1), the Cl^-(HCl) is not observed in either IMS or MS spectra. This is either because less HCl is produced in the ion source at the higher temperatures or because the Cl^-(HCl) ion thermally decomposes at higher temperatures prior to its passage into the drift region.

Another unexpected ion, $ClBr_2^-$, of drift time 64 ms is also noted in Figure 2 whenever *i*-PrBr has been added to the drift gas. This ion is thought to be produced by a reaction of some of the Cl^- ions with trace quantities of Br_2 in the ion source. Apparently, a trace amount of Br_2 is also produced by radiation chemistry within the ion source whenever small amounts of *i*-PrBr diffuse into the source region. The presence of this ion in subsequent IMS spectra can also be ignored, however, because this ion is stable and unreactive (as evidenced by its persistence in Figure 2F where a relatively large amount of *i*-PrBr has been added to the drift gas).

It would be very difficult to determine accurate rate constants for the S_N2 displacement reaction of interest from measurements of the type shown in Figure 2, and therefore, a different approach to such measurements will be described later. However, measurements of the type shown in Figure 2 do provide an excellent means of determining clustering equilibrium constants, K_1 and K_2, at any temperature of interest, as will be described in the following section.

Equilibrium Constants for Clustering. Numerous measurements, of the type shown in Figure 2, were made over the temperature range, 20−85 °C, where a significant shift in the observed drift time, t_{obs}, of the ion packet containing the Cl^- and Cl^-(*i*-PrBr) ions was caused by the successive addition of *i*-PBr to the drift gas. The t_{obs} values were then recorded as a function of the *i*-PrBr concentration added to the drift gas at each temperature, as illustrated in Figure 4 for a set of measurements made at 35 °C. Since the bare and clustered ions of Cl^- identified in Figure 3 were shown to have the same drift times and the same peak shapes, it can be assumed[7] that the equilibration time for cluster ion formation is very short compared with ionic drift times. Therefore, the observed drift

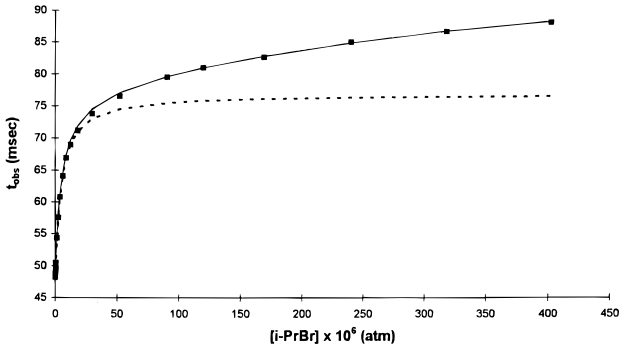

Figure 4. A typical measurement of the observed drift time, t_{obs}, for the Cl^--containing ion packet versus the concentration of *i*-PrBr added to the drift gas at a relatively low temperature, 35 °C. The dashed line indicates the t_{obs} values expected if only first-order clustering with $K_1 = 2.2 \times 10^5$ atm^{-1} were important, with K_2 assumed to be zero. The point at which the t_{obs} values begin to diverge from this dashed line indicates the onset of significant second-order clustering. The solid line indicates the t_{obs} values expected if both first- and second-order clustering are assumed to be important, with $K_1 = 2.2 \times 10^5$ atm^{-1} and $K_2 = 2.0 \times 10^3$ atm^{-1}. Excellent fit to all drift time measurements is then obtained.

times, $t_{obs,}$ can be expected[7] to be related to the equilibrium constants for the clustering reactions and the individual drift times of the bare and clustered Cl^- ions by the following set of relationships:

$$t_{obs} = t_0\alpha_0 + t_1\alpha_1 + t_2\alpha_2 \quad (5)$$

$$\alpha_0 = 1/(1 + K_1[i\text{-PrBr}] + K_1K_2[i\text{-PrBr}]^2) \quad (6)$$

$$\alpha_1 = K_1[i\text{-PrBr}]/D \quad (7)$$

$$\alpha_2 = K_1K_2[i\text{-PrBr}]^2/D \quad (8)$$

where t_i is the drift time expected for an individual Cl^- cluster ion containing *i i*-PrBr molecules, α_i is the fraction of ions under a mobility peak containing *i i*-PrBr molecules, K_i is the clustering equilibrium constant leading to the cluster ion $Cl^-(i\text{-PrBr})_i$, [*i*-PrBr] is the concentration of isopropyl bromide in the drift gas, and *D* is the denominator written in eq 6. Over the range of *i*-PrBr concentrations used in the present study, it will be shown that only cluster ions for which $i = 0$, 1, or 2 have significant relative abundance so that contributions of higher-order terms can be ignored.

Under conditions of relatively small [*i*-PrBr] and with the reasonable assumption that K_1 will be greater than all K_i of $i \geq 2$, eqs 5−8 can be combined[7] to form eq 9.

$$(t_{obs} - t_0)^{-1} = (K_1(t_1 - t_0)[i\text{-PrBr}])^{-1} + (t_1 - t_0)^{-1} \quad (9)$$

In Figure 5, the mobility data for the Cl^-/*i*-PrBr system at temperatures of 20, 40, and 60 °C have been plotted in the form $(t_{obs} - t_0)^{-1}$ vs $[i\text{-PrBr}]^{-1}$. In accordance with eq 9, a straight line is obtained over the range of measurements where [*i*-PrBr] is relatively small ($[i\text{-PrBr}]^{-1}$ is large). From the intercept of this line and from measurements of t_0 for Cl^- (in the absence of added *i*-PrBr), the single ion drift time, t_1, was obtained for the cluster ion, $Cl^-(i\text{-PrBr})_1$, at each temperature. Since the slopes of the lines shown in Figure 5 are expected (eq 9) to be equal to $(K_1(t_1 - t_0))^{-1}$, and the drift times, t_0 and t_1, have been determined, K_1 is obtained at each temperature. The uncertainty of the K_1 values thereby obtained is estimated to be no greater than ±20%. By the treatment of 15 data sets at 15 different temperatures, 15 K_1 values for the Cl^-/*i*-PrBr system were thereby determined and have been plotted in Figure 6 in the form of a van't Hoff plot. This log K_1 vs $1/T$ plot produces a straight line, as expected. By standard treatment[14] of the slopes and intercepts of these lines ($\ln K = -\Delta H/RT + \Delta S/R$), the standard enthalpy, $\Delta H°_1$, and standard entropy, $\Delta S°_1$, associated with the addition of one *i*-PrBr molecule to Cl^- is found to be $\Delta H°_1 = -13.6 \pm 1.0$ kcal mol^{-1} and $\Delta S°_1 = -20 \pm 3$ cal deg^{-1} mol^{-1}. These values, along with the corresponding value of $\Delta G°_1 = -7.6 \pm 0.1$ at 25 °C, are listed in Table 1. The only previous measurement of this equilibrium reaction is that of Caldwell *et al.*[13] by high-pressure mass spectrometry, who reported $K_1 = 3.9 \times 10^5$ atm^{-1} at a temperature of 304 K. From the $\Delta H°_1$ and $\Delta S°_1$ values determined here by IMS, K_1 is predicted to be 4.0×10^5 atm^{-1} at 304 K, in excellent agreement with the single measurement by Caldwell *et al.*

The dashed curve shown in Figure 4 is a prediction of t_{obs} obtained by eqs 5−8 using the values of t_0, t_1, and K_1 determined here and with the assumption that $K_2 = 0$. It is clear that, with

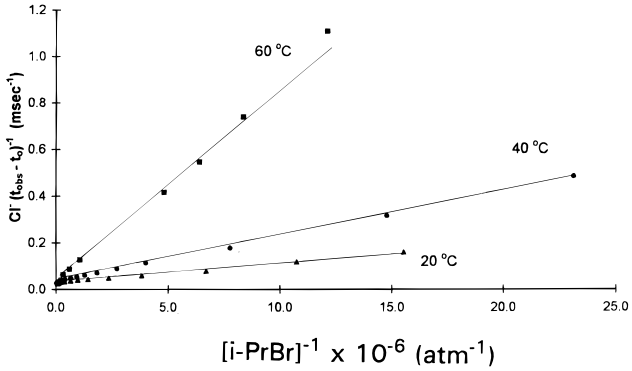

Figure 5. Changes in the drift time of the Cl^-/Cl^-(*i*-PrBr) ion packet as a function of *i*-PrBr concentration in the drift region, plotted in the form of eq 9. Equilibrium constants for the association of Cl^- with *i*-PrBr are determined from the intercepts and slopes of the least-squares lines thereby formed, as explained in the text.

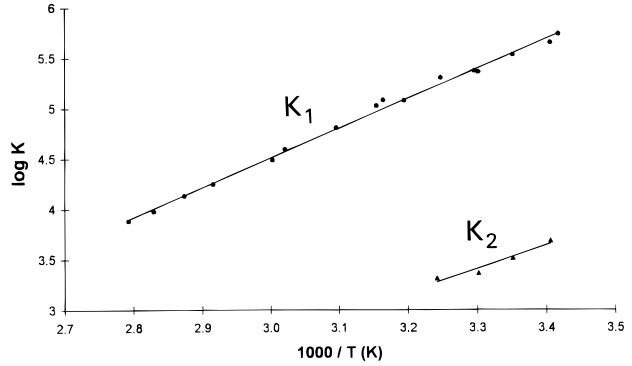

Figure 6. Van't Hoff plot of the equilibrium constants, K_1, for the association of Cl^- with *i*-PrBr over the temperature range 20−85 °C, and for the equilibrium constants, K_2, for the second-order clustering reaction, $Cl^-(i\text{-PrBr}) + i\text{-PrBr} = Cl^-(i\text{-PrBr})_2$, over the temperature range 20−36 °C as determined by reaction-modified IMS measurements.

TABLE 1: Thermodymanic Properties Determined by IMS for the Association of Chloride and Bromide Ions with Isopropyl Chloride and Isopropyl Bromide

reaction	$-\Delta H°$ [a]	$-\Delta S°$ [b]	$-\Delta G°_{298}$ [c]
$Cl^- + i$-PrBr	13.6	20	7.6
$Cl^- + i$-PrCl	12.9	20	7.1
$Br^- + i$-PrBr[d]	13.4	22	6.7
$Br^- + i$-PrCl	12.1	20	6.1

[a] Units are kcal mol^{-1}. Estimated uncertainty is ±1.0 kcal mol^{-1}. [b] Units are cal mol^{-1} K^{-1}. Estimated uncertainty is ±3 cal mol^{-1} K^{-1}. [c] Units are kcal mol^{-1}. Estimated uncertainty is ±0.1 kcal mol^{-1}. [d] Dougherty[24] previously reported $-\Delta H° = 12.2$ kcal mol^{-1}, $-\Delta S° = 20$ cal mol^{-1} K^{-1}, and $-\Delta G°_{298} = 6.3$ kcal mol^{-1} for this system.

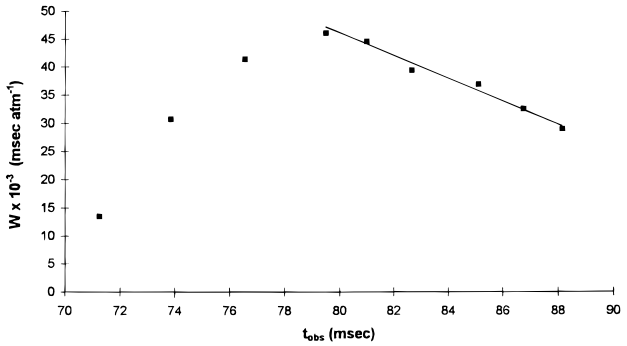

Figure 7. Drift time measurements for Cl^--containing ions observed in reaction-modified IMS spectra under conditions of relatively high *i*-PrBr concentration at 35 °C, plotted in the form of eq 10 where $W = (t_{obs} + t_{obs}K_1[i\text{-PrBr}] - t_0 - t_1K_1[i\text{-PrBr}])/K_1[i\text{-PrBr}]^2$. The slope of the straight line formed by t_{obs} measurements in excess of 80 ms provides a means of determining the equilibrium constant for second-order clustering, K_2.

this assumption of no clustering beyond the single cluster ion, good fit is observed only over a specific range of relatively low *i*-PrBr concentrations. With use of higher *i*-PrBr concentrations, both the t_{obs} values in Figure 4 and accompanying mass spectrometric measurements indicated that higher-order clustering, leading to the $Cl^-(i\text{-PrBr})_2$ ion, is also important. In order to determine the equilibrium constant, K_2, from these t_{obs} measurements, eq 10 can be used.[7]

$$W = -K_2t_{obs} + K_2t_2 \qquad (10)$$

where $W = (t_{obs} + t_{obs}K_1[i\text{-PrBr}] - t_0 - t_1K_1[i\text{-PrBr}])/K_1[i\text{-PrBr}]^2$. Equation 10 has also been derived from equations 5−8 under conditions of relatively high [*i*-PrBr] where second-order clustering is significant and with the assumption that $K_i = 0$ for all $i \geq 3$. (Note that all terms contributing to W are known). In Figure 7, the portion of the t_{obs} measurements at 35 °C (Figure 4) for which t_{obs} exceeded 70 ms has been plotted in the form W vs t_{obs}. In accordance with eq 10, a linear relationship is observed for the set of t_{obs} measurements in excess of about 80 ms where second-order clustering has become dominant. Analysis of the slope of this line leads to $K_2 = (2.0 \pm 0.4) \times 10^3$ atm^{-1} at 35 °C. The curve formed by the solid line in Figure 4 has been calculated from eqs 5−8 using values for t_0, t_1, t_2, K_1, and K_2 determined as described above from the graphical methods illustrated in Figures 5 and 7 (with the assumption that $K_i = 0$ for all $i \geq 3$). It is seen that this curve is in excellent agreement with all of the drift time measurements.

Measurements of K_2 were made over a narrow range of temperatures (20−36 °C), and these results are also shown in Figure 6 in the form of a van't Hoff plot. From the slope and intercept of this plot, $\Delta H°_2 = -7.8 \pm 2.2$ kcal mol^{-1} and $\Delta S°_2 = -10 \pm 6$ cal mol^{-1} K^{-1} are deduced for the addition of a second *i*-PrBr molecule to $Cl^-(i\text{-PrBr})$. A free energy change of $\Delta G°_2 = -4.8 \pm 0.1$ kcal mol^{-1} at 25 °C is also obtained.

Also listed in Table 1 are IMS equilibrium measurements made in the present study for the first-order clustering reactions, $Cl^- + i\text{-PrCl} = Cl^-(i\text{-PrCl})_1$, $Br^- + i\text{-PrBr} = Br^-(i\text{-PrBr})$, and $Br^- + i\text{-PrCl} = Br^-(i\text{-PrCl})$. For those cases where Br^- is the core ion, Br^- was made in the ion source by electron capture to CF_3Br, and the drift time of the Br^--containing ion packet was then monitored as a function of the concentration of either *i*-PrCl or *i*-PrBr added to the drift gas. The determination of these equilibrium constants from IMS spectra was relatively straightforward[7] because a simultaneous change in the core halide ion does not occur for these reaction systems either because an S_N2 displacement does not occur or because the S_N2 reaction system is symmetrical. The results summarized in

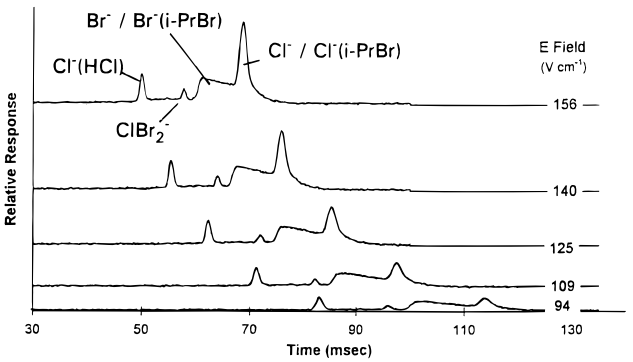

Figure 8. Typical reaction-modified IMS spectra from which rate constants were determined at relatively low temperature. By this procedure, the drift times of all ions are progressively increased by decreasing the electric field of the drift tube. The reaction time is defined to be equal to the drift time of the Cl^--containing ion packet. The relative contribution of the Cl^--containing ions to the IMS reaction-modified wave form is progressively decreased and that of Br^--containing ions is progressively increased as the reaction time is increased. Temperature is 35 °C.

Table 1 provide additional support for the accuracy of the K_1 determinations made here for the Cl^-/*i*-PrBr system from reaction-modified IMS spectra. While the four equilibrium systems have similar thermochemical parameters, a small but significant increase is noted in the magnitude of free energy change upon a change of the core anion from Br^- to Cl^-. A small increase is expected due to the smaller size of the Cl^- ion. Also, a small increase in the free energy change is noted upon changing the clustering agent from *i*-PrCl to *i*-PrBr. This result is consistent with the view that the greater polarizability expected for *i*-PrBr has a greater effect on the clustering interaction than the slightly greater acidity expected for the secondary hydrogen atom in *i*-PrCl.

Rate Constants for Nucleophilic Displacement Reactions. Rate constants for the S_N2 nucleophilic displacement reaction between Cl^- ion and *i*-PrBr were determined by measurements of the type illustrated in Figure 8. By this procedure, the reaction time (defined to be equal to the drift time of the Cl^-/$Cl^-(i\text{-PrBr})_i$ ion packet) is progressively increased by decreasing the electric field in the drift region. As is noted in Figure 8, the fraction of the IMS wave form that is due to the Cl^-/$Cl^-(i\text{-PrBr})_i$ ion packet is decreased, and the fraction of the IMS waveforn that is due to the $Br^-/Br^-(i\text{-PrBr})_i$ ion packet is increased as the reaction time is increased. The relative contribution of the reactant ion packet, containing Cl^- and $Cl^-(i\text{-PrBr})_i$ ions, to the total area of the reaction-modified IMS wave form was then determined by graphical analysis of each wave form,[6] and the magnitude of this quantity, called $A_{Cl}-/A_{total}$, was determined as a function of the reaction time.

In the analysis of these measurements, the following mathematical description of reaction sequence 4 has been applied. It is assumed that the sum of all Br^--containing product ions are formed by one or both of the two pathways shown in reaction 4. Therefore, the general rate law for the formation of product ions is given by

$$\mathrm{d(products)}/\mathrm{d}t = k_2[i\text{-PrBr}][Cl^-] + k_1[Cl^-(i\text{-PrBr})] \qquad (11)$$

Since the concentrations of the Cl^-, $Cl^-(i\text{-PrBr})$, and $Cl^-(i\text{-PrBr})_2$ ions are coupled by very fast equilibrium reactions, the following three relationships will also apply at all times:

$$K_1 = [Cl^-(i\text{-PrBr})]/[i\text{-PrBr}][Cl^-] \qquad (12)$$

$$K_2 = [Cl^-(i\text{-PrBr})_2]/[Cl^-(i\text{-PrBr})][i\text{-PrBr}] \qquad (13)$$

$$-\mathrm{d(products)}/\mathrm{d}t = \mathrm{d[Cl^-]}/\mathrm{d}t + \mathrm{d[Cl^-}(i\text{-PrBr})]/\mathrm{d}t + \mathrm{d[Cl^-}(i\text{-PrBr})_2]/\mathrm{dt} \quad (14)$$

The combination of these three equations leads to eq 15.

$$-\mathrm{d(products)}/\mathrm{d}t = \mathrm{d[Cl^-]}/\mathrm{d}t + K_1[i\text{-PrBr}]\,\mathrm{d[Cl^-]}/\mathrm{d}t + K_1K_2[i\text{-PrBr}]^2\mathrm{d[Cl^-]}/\mathrm{d}t \quad (15)$$

The combination of eqs 11 and 15 then provides the defining differential equation which, after integration over the reaction time, takes the following form:

$$([i\text{-PrBr}]^{-1} + K_1 + K_1K_2[i\text{-PrBr}])\ln([\mathrm{Cl^-}]_0/[\mathrm{Cl^-}]_t) = (k_2 + k_1K_1)t \quad (16)$$

where $[\mathrm{Cl^-}]_0$ is the initial $\mathrm{Cl^-}$ ion concentration and $[\mathrm{Cl^-}]_t$ is the $\mathrm{Cl^-}$ ion concentration remaining after reaction time, t. Since the ratio $[\mathrm{Cl^-}]_t/[\mathrm{Cl^-}]_0$, will be equal to the measured quantity $A_{\mathrm{Cl}}-/A_{\mathrm{total}}$ described above, eq 17 can be written:

$$Y = k_2't \quad (17)$$

where $Y = ([i\text{-PrBr}]^{-1} + K_1 + K_1K_2[i\text{-PrBr}])\ln(A_{\mathrm{total}}/A_{\mathrm{Cl}}-)$ and $k_2' = k_2 + k_1K_1$. (Note that the equilibrium constants K_1 and K_2 must be converted to units of $\mathrm{cm^3\ molecule^{-1}}$ prior to use in eq 17.) By eq 17, a plot of the known quantities, Y, vs time is expected to provide a straight line of slope equal to the sum of k_2 and k_1K_1, where K_1 is known from the equilibrium measurements described above. The sum of k_2 and k_1K_1 will be referred to here as the phenomenological second-order rate constant, k_2'. In Figure 9, plots of Y vs t for a range of reaction temperatures are shown. As expected, straight lines are observed in each case from which values of k_2' were determined from the slopes.

In Figure 10, the k_2' values obtained at all temperatures are shown (dots) in the form of an Arrhenius plot ($\log k_2'$ vs $1/T$). If viewed in the standard Arrhenius form $k = A\exp(-E_a/RT)$, the least-squares line formed by these k_2' measurements indicate a preexponential factor of $A = 5.0 \times 10^{-11}$ $\mathrm{cm^3\ s^{-1}}$ and an activation energy of $E_a = 1.4 \pm 0.3$ kcal $\mathrm{mol^{-1}}$. Also shown in Figure 10 (squares) are the determinations of k_2' for this reaction previously reported by Caldwell *et al.*[13] in 4 Torr of methane buffer gas and over a somewhat higher temperature range. While these two data sets indicate a moderate level of agreement at the common temperatures used, the line formed by the Caldwell measurements leads to significantly different Arrhenius parameters, $A = 1.2 \times 10^{-10}$ $\mathrm{cm^3\ s^{-1}}$ and $E_a = 5.6 \pm 0.5$ kcal $\mathrm{mol^{-1}}$, than those determined by the present IMS method. These differences in Arrhenius parameters suggest that different reaction mechanisms might be operative at the two buffer gas pressures, 4 and 640 Torr, used in these studies.

The possibility of a change to the E2 elimination mechanism, as shown by reaction 18, under one of the two conditions of buffer gas pressures has been considered.

$$\mathrm{Cl^-} + i\text{-PrBr} \rightarrow \mathrm{HCl} + \mathrm{CH_3CH{=}CH_2} + \mathrm{Br^-} \quad (18)$$

The E2 mechanism does not seem likely for a direct bimolecular interaction between $\mathrm{Cl^-}$ and *i*-PrBr due to the fact that reaction 18 would be endothermic by about 10 kcal $\mathrm{mol^{-1}}$ (deduced from known[15] heats of formation). If, on the other hand, reaction 18 proceeded through a thermalized ion complex, $\mathrm{Cl^-}(i\text{-PrBr})$, the reaction enthalpy of the first-order decomposition of this ion by the E2 elimination pathway would be even greater, about 23 kcal $\mathrm{mol^{-1}}$ (given by the enthalpy for reaction 18 less that of the $\mathrm{Cl^-}/i$-PrBr association reaction, listed in Table 1). Since

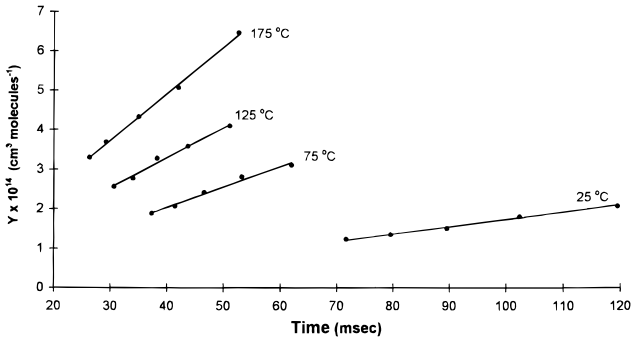

Figure 9. Extent of $\mathrm{Cl^-}$-containing reactant ion loss determined by IMS measurements vs reaction time for several temperatures, plotted in the form of eq 17. The slopes of the lines thereby formed provide a phenomenological second-order rate constant, $k_2' = k_2 + K_1k_1$, at each temperature. The concentrations of *i*-PrBr used at each temperature in order of increasing temperature are 7.3×10^{14}, 4.14×10^{13}, 5.89×10^{13}, and 2.43×10^{13} molecules $\mathrm{cm^{-3}}$.

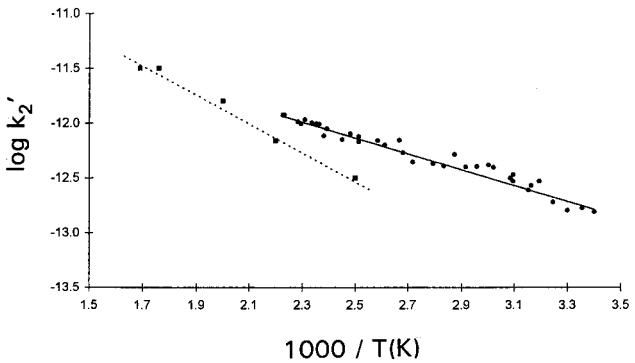

Figure 10. Phenomenological second-order rate constants, $k_2' = k_2 + K_1k_1$, for the reaction of chloride ion with isopropyl bromide determined here (dots) by IMS in atmospheric pressure nitrogen buffer gas and those reported by Caldwell *et al.* (squares) by PHPMS in 4 Torr of methane buffer gas, plotted in the Arrhenius form $\log k = \log A - (E_a/2.3RT)$. The estimated uncertainty of individual k_2' measurements in both studies is about ±20%.

the activation barrier for the observed decomposition of the $\mathrm{Cl^-}$-(*i*-PrBr) ion will be shown later to be significantly less than 23 kcal $\mathrm{mol^{-1}}$, an E2 reaction within a thermalized ion complex also does not appear to be possible.

It could be argued that the E2 reaction leads to the strongly hydrogen-bonded species, $\mathrm{Br^-(HCl)}$, instead of $\mathrm{Br^-}$ and HCl as shown in reaction 18. This would make the overall reaction about 15 kcal $\mathrm{mol^{-1}}$ more favorable and exothermic.[16] However, if the ion $\mathrm{Br^-(HCl)}$ was a product of an E2 reaction, it would be stable and observable under the relatively low-temperature conditions of the IMS used here. This ion was not observed here under low-temperature conditions (see Figure 3).

Having ruled out the possibility of a change to a distinctly different E2 mechanism, consideration will now be given to the feasibility of more subtle expected effects of pressure that could alter the detailed means by which an S_N2 displacement reaction proceeds at the two pressures represented in Figure 10.

Associated Rate Measurements at Lower Pressures. In assessing the relative importance of the direct S_N2 reaction (k_2) and the indirect mechanism (k_1K_1) in determining the displacement mechanism, it is useful to consider more closely the present results and those of Caldwell *et al.*,[13] shown in Figure 10. In both studies, a second-order rate constant is obtained that is expected to be equal to the phenomenological second-order constant, $k_2' = k_2 + k_1K_1$, under each of the two reaction conditions. The fact that the Arrhenius parameters that define the two sets of rate constants in Figure 10 are significantly

different implies that the mechanisms are not exactly the same under the two conditions of buffer gas pressure. Therefore, it might be suggested that the direct displacement reaction (k_2) was more important and the indirect mechanism (k_1K_1) was less important in the study of Caldwell *et al*. performed at relatively low pressures than in the present study.

In considering the relative importance of the direct and indirect displacement mechanisms, it is necessary to view these processes in somewhat greater detail, as in reaction 19.

$$\mathrm{Cl^-} + i\text{-PrBr} \underset{k_b}{\overset{k_c}{\rightleftharpoons}} (\mathrm{Cl^-} \bullet i\text{-PrBr})^* \xrightarrow{k_B[B]} \mathrm{Cl^-}(i\text{-PrBr}) \qquad (19)$$

$$(\mathrm{Cl^-} \bullet i\text{-PrBr})^* \xrightarrow{k_p} \text{products}$$

The production of Br^--containing products by the direct displacement mechanism will proceed through a short-lived excited intermediate, $(Cl^- \cdot i\text{-PrBr})^*$, whose rate of formation is determined by the collisional rate constant, k_c, and whose rate of destruction is determined by the sum of three rate constants: k_p for formation of the displacement product, k_b for back-dissociation of the excited ion complex, and $k_B[B]$ for the collisional stabilization of the intermediate by the buffer gas, B. The overall rate constant, k_2, for the direct S_N2 displacement reaction will be given by

$$k_2 = k_c k_p (k_p + k_b + k_B[B])^{-1} \qquad (20)$$

Since the reaction under consideration is very much slower than the collision rate under all reaction conditions, it can be assumed that $k_p \ll k_b + k_B[B]$ under all conditions. Therefore, eq 20 can be rewritten in the form

$$k_2 = (k_c k_p / k_b)/(1 + k_B[B]/k_b) \qquad (21)$$

where the effect of buffer gas pressure change on k_2 will be provided by the unitless collective term, $k_B[B]/k_b$.

With a pulsed high-pressure mass spectrometer,[17,18] we have been able to measure the collective term, $k_B[B]/k_b$, for the closely related reaction system involving Cl^- ion and isopropyl chloride (*i*-PrCl) in methane buffer gas at a pressure of 0.5 Torr at room temperature. The mechanism for the forward association reaction of Cl^- and *i*-PrCl is analogous to that shown in reaction 19. However, since any displacement reaction that might occur causes no net change in the identity of the halide ion, this reaction system can be expressed as follows:

$$\mathrm{Cl^-} + i\text{-PrCl} \underset{k_b}{\overset{k_c}{\rightleftharpoons}} (\mathrm{Cl^-} \cdot i\text{-PrCl})^* \xrightarrow{k_B[B]} \mathrm{Cl^-}(i\text{-PrCl}) \qquad (22)$$

The rate constant k_{assoc} for this reaction will be given by

$$k_{assoc} = k_c k_B[B]/(k_b + k_B[B]) \qquad (23)$$

which can be rearranged to form

$$k_{assoc}/k_c = (k_B[B]/k_b)/(1 + k_B[B]/k_b) \qquad (24)$$

Our PHPMS measurements of this reaction system (with 1.0 mTorr of *i*-PrCl in 0.50 Torr of methane buffer gas at 25 °C) indicate that a state of clustering equilibrium is reached after about 500 μs. Analysis of the rate at which this equilibrium condition is reached, using the standard equations for relaxation processes,[19] indicated that $k_{assoc} = (1.5 \pm 0.5) \times 10^{-11}$ cm^3 s^{-1} under these conditions. A collision rate constant of $k_c = 1.8 \times 10^{-9}$ cm^3 s^{-1} is deduced from ADO theory.[20] By eq 24, $k_B[B]/k_b \approx 0.008$ is thereby deduced for this reaction system at a pressure of 0.5 Torr. Therefore, in a buffer gas of 4 Torr of methane, as was used in the study of Caldwell *et al*.[13] for study of the reaction of Cl^- with *i*-PrBr, $k_B[B]/k_b$ might be expected to be equal to $\approx$0.06, from which $k_2 \approx 0.95(k_c k_p/k_b)$ is predicted by eq 21. In a nitrogen buffer gas of 640 Torr, as is used in the present IMS studies of the reaction of Cl^- with *i*-PrBr, $k_B[B]/k_b \approx 10$ would be expected (assuming the efficiency of collisional quenching is the same for methane and nitrogen), from which $k_2 \approx 0.10(k_c k_p/k_b)$ is predicted by eq 21. From these considerations, one might expect that k_2 would decrease by about 1 order of magnitude, with a pressure change from 4 to 640 Torr. This, of course, would greatly increase the importance of the direct S_N2 mechanism under the lower pressure conditions used by Caldwell *et al*. and would greatly decrease its importance in the present study.

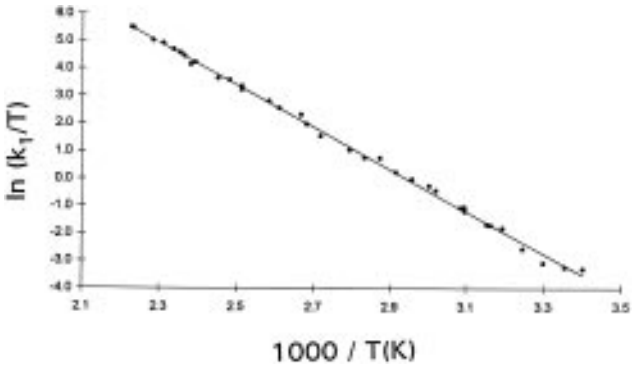

Figure 11. First-order rate constant, k_1, for conversion of the thermal energy ion complex, Cl^-(*i*-PrBr), to Br^--containing products determined from the present IMS measurements at atmospheric pressure over the temperature range 20−175 °C.

In addition, the discussion of reaction 22 indicates that the use of lower buffer gas pressures would decrease the rate of the forward clustering reaction that has been shown here to lead to a condition of clustering equilibrium within the IMS at atmospheric pressure. Therefore, under the lower pressure conditions of Caldwell *et al*.,[13] it is much more likely than in the present study that the rates of the forward clustering reactions are not sufficiently fast so as to maintain a condition of true equilibrium. In that case a steady-state condition of clustering that is short of the true equilibrium position would be achieved. This would cause the rate constant for the indirect mechanism to be less than the product term, k_1K_1, and would additionally increase the relative importance of the direct mechanism at lower pressures.

In view of the above considerations, it is reasonable to suggest that the dominant mechanism for the S_N2 displacement reaction studied here under conditions of atmospheric pressure is the indirect mechanism for which the observed rate constant k_2' is equal to the product of k_1 and K_1.

Enthalpy of Activation for S_N2 Displacement within the Ion Complex. In Figure 11, rate constants k_1 determined here from the relationship $k_1 = k_2'/K_1$ have been plotted in the form, $\ln(k_1/T)$ vs $1/T$ (K). A plot of this form is expected to provide a straight line for gas phase unimolecular processes in which the reactant is maintained in a continuous state of thermal equilibrium with the medium ($k_1/T = (k/h)\exp(\Delta S^{\pm}/R)\exp(-\Delta H^{\pm}/RT)$, where $\Delta S^{\pm}$ and $\Delta H^{\pm}$ are the entropy and enthalpy of activation[21]). From the slope of this line, $\Delta H^{\pm} = 15.2$ kcal mol^{-1} and $\Delta S^{\pm} = -2.2$ cal mol^{-1} K^{-1} are deduced for the unimolecular decomposition of the thermal energy ion complex to form Br^--containing product ions. The combination of this $\Delta H^{\pm}$ measurement with the measurements of the enthalpy of clustering equilibria reported in Table 1 allows the potential energy surface shown in Figure 12 to be constructed. The energy of the products indicated in this figure have been calculated from the known electron affinities of the chlorine

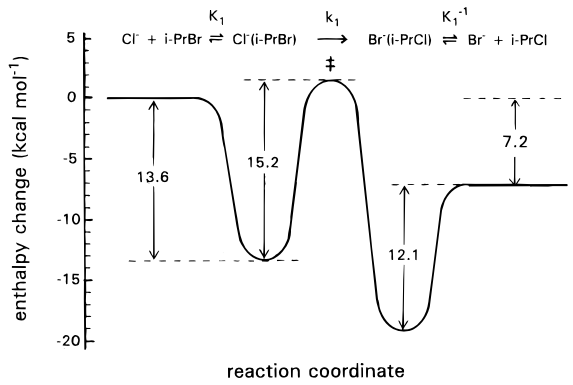

Figure 12. Principal energy changes along the Cl^-/*i*-PrBr reaction coordinate. The first three magnitudes indicated in the figure have been determined here by IMS measurements of rate constants, k_1, and equilibrium constants, K_1. These measurements place the S_N2 transition state for this reaction at 1.6 kcal mol^{-1} above the energy of the reactants. The enthalpy of the final products has been calculated from known thermochemical data.

(83.4 kcal mol^{-1} [22]) and bromine (77.6 kcal mol^{-1-1} [22]) atoms and the known C−Cl and C−Br bond energies of *i*-PrCl (81 kcal mol^{-1-1} [23]) and *i*-PrBr (68 kcal mol^{-1-1} [23]) while assuming that all C−H and C−C bonds within *i*-PrCl and *i*-PrBr are the same. From the present IMS measurements, it is therefore concluded that the energy of the S_N2 transition state for the reaction of chloride with isopropyl bromide lies about 1.6 kcal mol^{-1} above that of the reactants. Corresponding IMS measurements made previously in our laboratory for the reactions of chloride ion with methyl bromide, ethyl bromide, and *n*-butyl bromide placed the S_N2 transition states for those reactions at 2.2, 0.0, and 1.3 kcal mol^{-1}, respectively, below the energies of the reactants. The higher transistion state energy observed here for the reaction of chloride with isopropyl bromide can be attributed to increased steric hindrance to backside attack for this secondary alkyl bromide.

Conclusions

In this study, the relatively complex nucleophilic S_N2 displacement reaction of the chloride ion with isopropyl bromide has been studied in nitrogen buffer gas at 640 Torr between 20 and 175 °C by ion mobility spectrometry. Under the conditions existing within the IMS, a prior clustering reaction between the two reactants occurs sufficiently rapidly that a state near that of the true clustering equilibrium condition is continuously maintained. This allows the energetics of this process to be accurately characterized while a slower S_N2 displacement reaction is simultaneously occurring. As a result, both processes can be quantitatively characterized from reaction-modified IMS spectra. Analysis of the present IMS results are greatly facilitated by the fact that reaction intermediates, as well as reactants, tend to be maintained in a state of physical equilibrium with the buffer gas medium when unusually high buffer gas pressures are used.

It has been shown that under these conditions the S_N2 nucleophilic displacement reaction probably occurs by the following distinctly two-step mechanism

$$Cl^- + i\text{-PrBr} \overset{K_1}{\rightleftharpoons} Cl^-(i\text{-PrBr}) \overset{k_1}{\longrightarrow} Br^- + i\text{-PrCl} \quad (25)$$

in which a thermalized ion complex, Cl^-(*i*-PrBr), is maintained in a state of chemical equilibrium with the reactants. An S_N2 displacement reaction then occurs within the cluster ion by its unimolecular decomposition to Br^--containing product ions. By measurements of the associated equilibrium constants, K_1, and rate constants, k_1, as a function of temperature, the enthalpy changes associated with each of the two steps have been determined and place the energy of the S_N2 transition state for this reaction at 1.6 kcal mol^{-1} above that of the reactants.

The experimental method demonstrated here for the study of gas phase ion−molecule reactions is made additionally significant by recent theoretical treatments of gas phase S_N2 displacement reactions in which the association complexes resulting from the attachment of chloride ion to methyl chloride[25] and to methyl bromide[26] were predicted to behave in very complex and distinctly non-statistical manners. Such behavior would greatly complicate all attempts to interpret rate constants for ion−molecule reactions of this type if the rate constants were measured under conditions of relatively low pressure where the association complexes are isolated during their lifetimes. Therefore, techniques such as described here, where very high buffer gas pressure causes all reaction intermediates to be brought into a state of thermal equilibrium with the medium, might provide the only means of obtaining macroscopic rate constants that can be reliably interpreted in terms of the potential energy surfaces for dynamically complex ion−molecule reactions of this type.

Acknowledgment. The authors thank D. A. Williamson for providing PHPMS measurements. This work was supported by a grant from the Chemistry Division of the National Science Foundation (CHE-9509330).

References and Notes

(1) Knighton, W. B.; Grimsrud, E. P. In *Advances in Gas Phase Ion Chemistry;* Adams, N. G., Babcock, L. M., Eds.; JAI Press: Greenwich, CN, 1996; Vol. 2, pp 219−256.

(2) Cacace, F. *Acc. Chem. Res.* **1988**, *21*, 215−222.

(3) Cacace, F. *Science* **1990**, *250*, 392−399.

(4) Speranza, M. *Mass Spectrom. Rev.* **1992**, *11*, 73−117.

(5) Speranza, M. *Int. J. Mass Spectrom. Ion Processes* **1992**, *118/119*, 395−447.

(6) Giles, K.; Grimsrud, E. *J. Phys. Chem.* **1992**, *96*, 6680−6687.

(7) Giles, K.; Grimsrud, E. P. *J. Phys. Chem.* **1993**, *97*, 1318−1323.

(8) Knighton, W. B.; Bognar, J. A.; O'Connor, P. M.; Grimsrud, E. P. *J. Am. Chem. Soc.* **1993**, *115*, 12079−12084.

(9) Bohme, D. K.; Raksit, A. B. *Can. J. Chem.* **1985**, *63*, 3007.

(10) Henchman, M.; Paulson, J. F.; Hierl, P. M. *J. Am. Chem. Soc.* **1983**, *105*, 5509.

(11) Hierl, P. M.; Ahrens, A. F.; Henchman, M.; Viggiano, A. A.; Paulson, J. F. *J. Am. Chem. Soc.* **1986**, *108*, 3142−3143.

(12) Henchman, M.; Hierl, P. M.; Paulson, J. F. *Adv. Chem. Ser.* **1987**, *215*, 83−101.

(13) Caldwell, G.; Magnera, T. F.; Kebarle, P. *J. Am. Chem. Soc.* **1984**, *106*, 959−966.

(14) Kebarle, P. *Annu. Rev. Phys. Chem.* **1977**, *28*, 445−476.

(15) Dean, J. A. *Lange's Handbook of Chemistry*; McGraw-Hill: New York, 1992; p 6.5.

(16) Yamdagni, R.; Kebarle, P. *Can. J. Chem.* **1977**, *52*, 2449.

(17) Knighton, W. B.; Grimsrud, E. P. *J. Am. Chem. Soc.* **1992**, *114*, 2336−2342.

(18) Knighton, W. B.; Bognar, J. A.; Grimsrud, E. P. *J. Mass Spectrom.* **1995**, *30*, 557−562.

(19) Laidler, K. J. *Chemical Kinetics*; McGraw-Hill Book Co.: New York, 1965; p 24.

(20) Su, T.; Bowers, M. T. *Gas Phase Ion Chemistry*; Bowers, M. T., Ed.; Academic Press: New York, 1979; p 83.

(21) Laidler, K. J. *Chemical Kinetics*; McGraw-Hill Book Co.: New York, 1965; p 123.

(22) Weast, R. C.; Astle, M. J.; Beyer, W. H. *CRC Handbook of Chemistry and Physics*; CRC Press: Boca Raton, FL, 1988; p F-198.

(23) Weast, R. C.; Astle, M. J.; Beyer, W. H. *CRC Handbook of Chemistry and Physics*; CRC Press: Boca Raton, FL, 1988; p E-64.

(24) Dougherty, R. C. *Org. Mass Spectrom.* **1974**, *8*, 85.

(25) Vande Linde, S. R.; Hase, W. L. *J. Phys. Chem.* **1990**, *94*, 6148.

(26) Wang, H.; Peslherbe, G. H.; Hase, W. L. *J. Am. Chem. Soc.* **1994**, *116*, 9644.